LETTER

Encoding of action by the Purkinje cells of the cerebellum

David J. Herzfeld[1], Yoshiko Kojima[2], Robijanto Soetedjo[2] & Reza Shadmehr[1]

Execution of accurate eye movements depends critically on the cerebellum[1–3], suggesting that the major output neurons of the cerebellum, Purkinje cells, may predict motion of the eye. However, this encoding of action for rapid eye movements (saccades) has remained unclear: Purkinje cells show little consistent modulation with respect to saccade amplitude[4,5] or direction[4], and critically, their discharge lasts longer than the duration of a saccade[6,7]. Here we analysed Purkinje-cell discharge in the oculomotor vermis of behaving rhesus monkeys (_Macaca mulatta_)[8,9] and found neurons that increased or decreased their activity during saccades. We estimated the combined effect of these two populations via their projections to the caudal fastigial nucleus, and uncovered a simple-spike population response that precisely predicted the real-time motion of the eye. When we organized the Purkinje cells according to each cell's complex-spike directional tuning, the simple-spike population response predicted both the real-time speed and direction of saccade multiplicatively via a gain field. This suggests that the cerebellum predicts the real-time motion of the eye during saccades via the combined inputs of Purkinje cells onto individual nucleus neurons. A gain-field encoding of simple spikes emerges if the Purkinje cells that project onto a nucleus neuron are not selected at random but share a common complex-spike property.

Previous studies have focused on bursting activity of Purkinje cells during saccadess[6,10,11] and found no consistent modulation with saccade amplitude[4,5], speed[5–7] or direction[4]. A recent simulation[12] suggested that Purkinje cells that pause during saccades may be important in understanding the responses observed in the deep cerebellar nucleus neurons. The main question that we wished to address was how the Purkinje cells encode the real-time motion of the eye.

We analysed simple-spike activity of 72 Purkinje cells in the oculomotor vermis (OMV, cerebellar lobules VI and VII) of five monkeys during saccades. The population included cells that exhibited increased activity (bursting; $n = 39$, Fig. 1a) or decreased activity (pausing; $n = 33$, Fig. 1b). Consistent with previous reports[5,6,10], most neurons were poorly modulated by saccade amplitude (Fig. 1c and Extended Data Fig. 1); however, the mean firing rate of burst cells (but not pause cells) increased significantly with saccade peak speed (Fig. 1d, $P < 10^{-10}$). Previous work had demonstrated that the population response encoded additional saccade-related information that was not reliably present in the responses of individual neurons[6,13,14]. To examine the population response, we measured change in firing rates (from baseline) for the bursting and pausing cells during slow ($400°\ s^{-1}$) and fast ($650°\ s^{-1}$) saccades (Fig. 1e), pooled across all directions. The onset of change in firing rates in both populations generally led saccade onset by more than 50 ms. The termination of activity was also significantly later than the saccade: a $650°\ s^{-1}$ saccade was 38 ± 1.2 ms in duration (mean ± s.e.m.), whereas activity of burst and pause cells persisted for more than 100 ms. Given that the cerebellum is thought to have a critical role in termination of ipsiversive saccades[15,16], it is unlikely that separate populations of burst or pause Purkinje cells control the motion of the eye, since their activity persists for much longer than the saccade.

Purkinje cells project to the caudal fastigial nucleus (cFN), where about 50 Purkinje cells converge onto a cFN neuron[17]. For each Purkinje cell we computed the probability of a simple spike in 1-ms time bins during saccades of a given peak speed, averaged across all
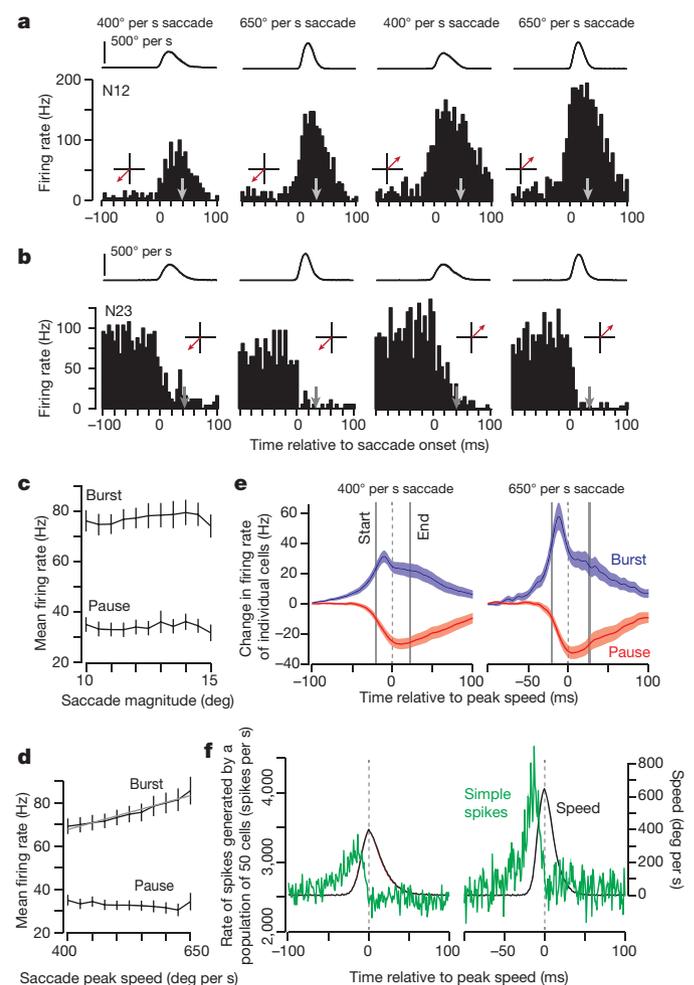
Figure 1 | Population of burst and pause Purkinje cells together predict eye speed in real time. a, b, Perisaccade histograms for a bursting (**a**) and pausing (**b**) Purkinje cell during saccades of various speeds and directions (red arrow). The trace on the top row is saccade speed. The grey arrow indicates saccade end. **c, d**, Mean firing rates over the duration of saccade computed across all directions. Changes in speed produced an increase in the firing rate of the burst cells but not the pause cells. **e**, Change in firing rates (with respect to baseline) of the bursting and pausing Purkinje cells for two saccade speeds. Grey bars are onset and termination of the saccade (width is s.e.m.). **f**, The total rate of simple spikes produced by a random selection of 50 Purkinje cells.

[1]Department of Biomedical Engineering, Laboratory for Computational Motor Control, Johns Hopkins University School of Medicine, Baltimore, Maryland 21205, USA. [2]Department of Physiology and Biophysics, Washington National Primate Center, University of Washington, Seattle, Washington 98195, USA.

directions. We then chose 50 Purkinje cells at random and computed the total number of simple spikes generated by the population at each millisecond, resulting in an estimate of the rate of presynaptic spikes converging onto a cFN cell. The results (Fig. 1f) revealed a real-time encoding of the speed of the eye: the peak of the activity preceded peak speed, increased in magnitude when speed increased, and returned to baseline just before saccade termination (R^2 at the optimal delay, $400°\,s^{-1}$: $R^2 = 0.52$, $P < 10^{-22}$; $650°\,s^{-1}$: $R^2 = 0.62$, $P < 10^{-43}$). It appeared that the simple spikes of the pause and burst cells combined together to predict motion of the eye.

Let us hypothesize that the Purkinje cells that project to a nucleus neuron are not selected randomly, but are organized by their inputs from the inferior olive[18]. That is, suppose that the olive projections divide the Purkinje cells into clusters where each cluster of Purkinje cells projects onto a single nucleus neuron. The input from the olive produces complex spikes in the Purkinje cells. We found that if we organized the simple spikes of the Purkinje cells based on each cell's complex-spike properties, additional features of the population activity were unmasked.

We measured complex-spike properties of each Purkinje cell by inducing a post-saccadic error through displacement of the target during the saccade, and then measured the probability of complex spikes as a function of the direction of this error (Fig. 2 and Supplementary Information section 2). For each Purkinje cell, the direction of error that produced the largest probability of complex spikes during the 50–200-ms post-saccade period was labelled as CS-on, and the opposite direction was labelled as CS-off[9] (Extended Data Fig. 2). We then made the assumption that the Purkinje cells that projected onto a nucleus neuron all had the same CS-on direction (Fig. 3a). Under this assumption, we computed the rate of presynaptic simple spikes that a nucleus neuron would receive from the cluster of Purkinje cells (Supplementary Information section 3). We did this by convolving each Purkinje cell simple-spike train with a 2.5 ms standard-deviation normalized Gaussian, approximating the temporal characteristics of the inhibition produced in the nucleus neuron due to a simple spike in the Purkinje cell[17,19].

Figure 3b shows the change in population response from the baseline level when a saccade was made in the same direction as CS-off. The response rose above baseline before saccade onset, peaked before peak speed, and then returned to near baseline. The peak response scaled robustly with saccade amplitude (Fig. 3c, $R^2 = 0.93$, $P < 10^{-5}$). We observed a strong correspondence between the real-time population response and the real-time speed (Fig. 3d, lower plot, and Extended Data Fig. 3). The population response preceded eye speed by an average of 21.2 ± 0.4 ms (correlation analysis in the CS-off direction, mean ± s.e.m.). Peak population response precisely predicted peak speed (Fig. 3e, $R^2 = 0.98$, $P < 10^{-7}$).

We took advantage of natural variability in saccades to test further the relationship between the population response and speed. We sorted all $10°$ saccades (direction CS-off) according to peak speed (Fig. 3f) and found that despite the constant amplitude, the population response precisely predicts the actual peak speed of the eye (Fig. 3g, $R^2 = 0.96$, $P < 10^{-7}$). Therefore, when the simple spikes were organized according to each cell's complex-spike directional preference, the population response for saccades of constant direction predicted nearly all of the variability in saccade peak speed.

No previous work, to our knowledge, had revealed how direction of a saccade is encoded in the activity of Purkinje cells. For the burst and pause cells, the mean and peak firing rates during the saccade did not vary as a function of direction (Extended Data Fig. 4). However, organizing the population response according to each Purkinje cell's complex-spike tuning preference revealed a clear encoding of direction: the peak response was greater if the saccades were in the same direction as CS-off as compared to CS-on (Fig. 4a, t-test, $P < 10^{-16}$). Indeed, the peak population response rose linearly as a function of peak speed in both directions, but with a larger gain when the saccade direction was congruent with CS-off (Fig. 4b,
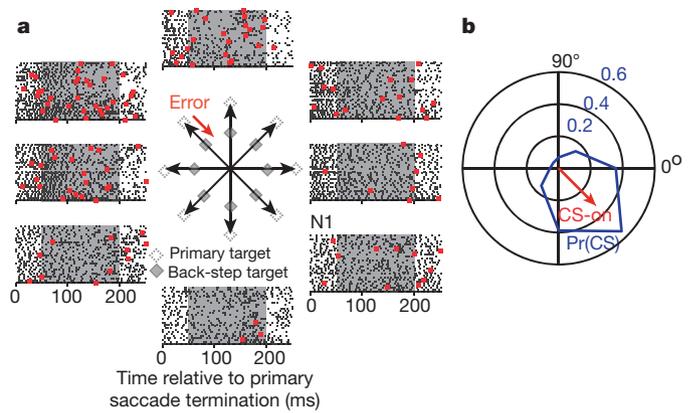
Figure 2 | Determination of complex-spike properties of Purkinje cells. **a**, Response of a Purkinje cell during the 250-ms period after completion of a saccade (simple spikes are grey; complex spikes are red). CS-on was determined via a back-step paradigm in which the target was jumped (unfilled target to filled target) during saccade execution. Black arrow indicates saccade vector, red arrow indicates error vector. We computed the probability of complex spikes in the 50–200-ms period after saccade termination. **b**, The probability of a complex spike (Pr(CS)) as a function of the direction of the error vector. For this neuron, the highest probability (CS-on) occurred when the error vector was in direction $-45°$. The direction of CS-off for this cell was $135°$.

repeated measures analysis of variance (ANOVA) with main effects of peak speed, $P < 10^{-15}$; CS-direction $P < 10^{-7}$; and a speed by CS-direction interaction, $P < 10^{-15}$).

To examine the effects of saccade direction more closely, we plotted the population response across saccade directions with respect to CS-on (Fig. 4c). We found that the population response was highest for saccades made in the CS-off direction, with an encoding of direction that resembled a cosine function (Fig. 4d). Therefore, the combined activity of burst and pause cells, but not the activity of either population individually (Extended Data Fig. 4), aligned to CS-off, produced a population response that exhibited gain-field encoding: the magnitude of the population response increased linearly with speed, and was cosine-tuned in direction, with a multiplicative interaction between speed and direction. The rate of simple spikes converging onto cFN, represented by $s(t)$, predicted in real-time motion of the eye (Supplementary Information section 4 and Extended Data Fig. 5) is:

$$s(t) = |\dot{x}(t+\Delta)|g(\theta, \theta_{CS}) + c$$
$$g(\theta, \theta_{CS}) = a\cos(\theta - \theta_{CS}) + b \tag{1}$$

In equation (1), $|\dot{x}(t+\Delta)|$ represents the magnitude of the eye velocity vector (the time derivative of eye position, x) at time $t + \Delta$ (where $\Delta = 19$ ms), b and c are baseline offsets, a is a scaling factor, θ is saccade direction, and θ_{CS} is direction of CS-off for that cluster of Purkinje cells. The resulting gain-field encoding of eye motion is depicted in Fig. 4e.

We next addressed the question of how the activity of individual cells produced this directional encoding in the population response. The main contributors were the pause cells, which started their pause approximately 10 ms earlier when the saccade was in the CS-on direction (Fig. 4f), a change that was independent of saccade speed (Extended Data Fig. 6). This subtle shift in the timing of spikes produced an increase of the population response when saccade direction changed from CS-on to CS-off (Fig. 4a).

We found that the anatomical distribution of Purkinje cells, as labelled by their CS-off direction, was not random, but lateralized[9] (Extended Data Fig. 7), confirming previous anatomical studies suggesting that olivary projections are contralateral[20,21]. Purkinje cells with rightward CS-off were more likely to be on the right side of the cerebellum (t-test, $P < 10^{-4}$). This indicates that saccades made in the same direction as CS-off were typically ipsiversive, whereas saccades

Figure 3 | A cluster of Purkinje cells, organized by their complex spikes, produced a population response that predicted in real time the motion of the eye. a, Hypothesized organization of the oculomotor vermis. To compute a population response, we measured the simple spikes of each Purkinje cell as a function of saccade direction with respect to the CS-on direction of that cell. For the Purkinje cells shown here, the CS-on is an error vector to the left (arrow). **b**, Change in population response (with respect to baseline) as a function of saccade amplitude in 0.5° bins, for saccades in the CS-off direction. Data in the amplitude axis were smoothed by a first-order Savitzky–Golay filter with a width of three bins[6]. Bottom plot shows the population response for three representative amplitudes. **c**, Peak population response increased linearly with saccade amplitude. P values indicate significant linear correlation. **d**, Population response as a function of saccade peak speed. Bottom plot shows representative responses with their corresponding speed traces. **e**, Peak population response increased linearly with saccade peak speed. **f**, Population response for 10° saccades (±1°), as a function of saccade peak speed. Bottom plot shows the population response for slow, medium and fast saccades of 10° amplitude. **g**, Peak population response increased linearly as a function of peak speed even for a fixed magnitude saccade. Error bars are s.e.m.
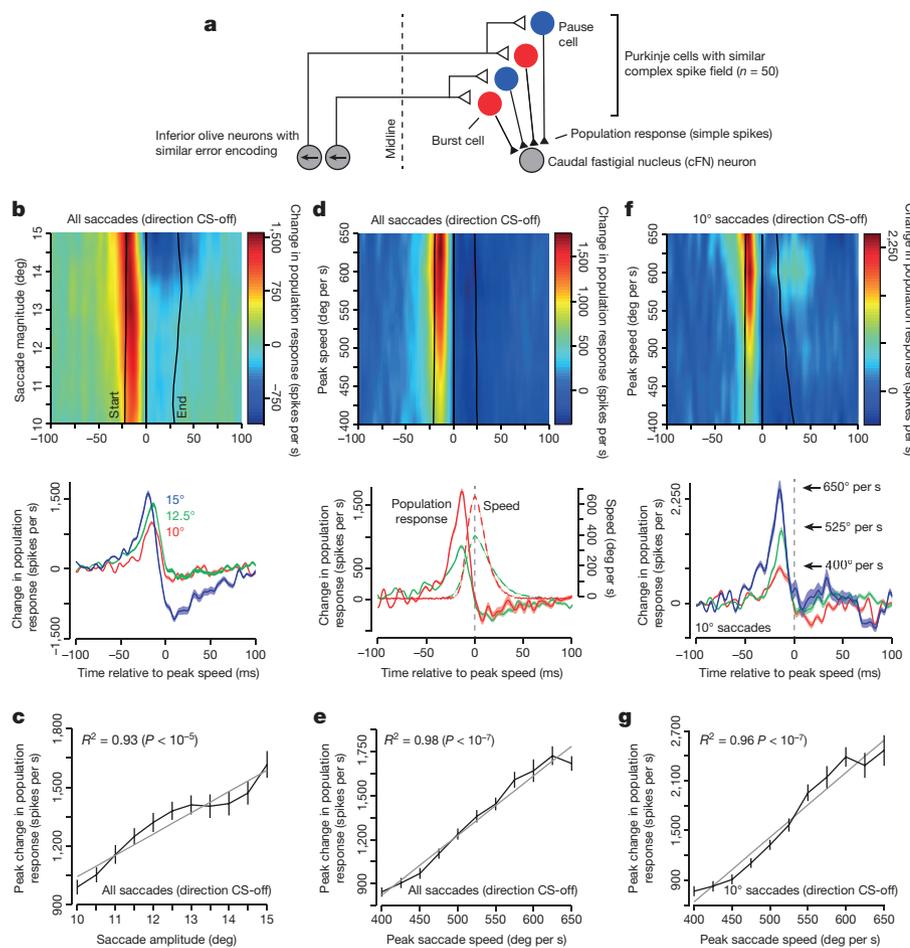
congruent with CS-on were contraversive. In contrast, pause and burst cells were uniformly distributed across the cerebellum ($P > 0.4$).

Our results rely critically on our hypothesis that Purkinje cells organize into clusters with roughly equal numbers of pause and burst cells, all with a common complex-spike tuning preference (Fig. 3a). If, contrary to our hypothesis, pause and burst cells organized into separate clusters, the population response would not predict the real-time motion of the eye (Fig. 1e). Similarly, if each cluster was not
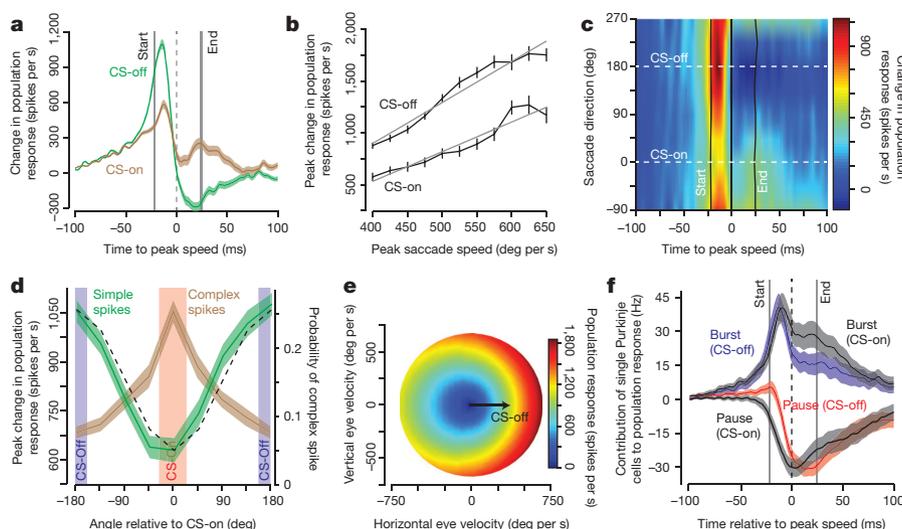
Figure 4 | Population response of Purkinje cells predicted saccade speed and direction in real time as a gain field. a, Population response for saccades in direction CS-on and CS-off. The population response is larger when the saccade is in the CS-off direction. **b**, Peak population response grew linearly with saccade speed, but had a higher gain for saccades in the CS-off direction. **c**, Real-time population response as a function of saccade direction relative to CS-on. Data smoothed as in Fig. 3b. **d**, Peak population response (labelled as simple spikes) as a function of saccade direction with respect to CS-on. The brown curve shows probability of observing a complex spike as a function of the angle relative to each neuron's CS-on. The black curve indicates cosine fit of the peak population response. **e**, Gain-field encoding by a cluster of Purkinje cells whose CS-off direction is to the right (equation (1)). **f**, Contribution of single Purkinje cells to the population response. A change in direction coincides with a shift in timing of the pause cells. Error bars are s.e.m.

composed of roughly equal numbers of pause and burst cells, the population response could not predict the real-time speed of the eye (Extended Data Fig. 8 and Supplementary Information section 5). The fact that burst and pause cells were distributed uniformly across the recording locations, and not lateralized as we found with the complex-spike tuning properties, suggests that a cluster is composed of both burst and pause. Finally, if we ignored the complex-spike properties of the Purkinje cells, and made the typical assumption that simple spikes were sufficient to uncover the coordinate system of encoding motion, then the gain-field representation of speed and direction would disappear (Extended Data Fig. 9 and Supplementary Information section 6).

Organizing the Purkinje cell into clusters where all the cells shared a common complex-spike property resulted in simple spikes that encoded speed and direction in real time via a gain field.

Together, our results suggest three principles of cerebellar function during control of saccadic eye movements. First, the cerebellum predicts real-time motion not in the time course of individual Purkinje cell simple spikes, nor in the individual activities of the bursting or pausing populations, but in the combined activities of these two populations via the simple spikes that converge onto cells in the deep cerebellar nucleus. A similar population coding has been suggested during smooth pursuit[22]. Second, this population input to each nucleus neuron encodes direction and speed via a gain field. Because a similar encoding has been shown in the posterior parietal cortex during saccades[23], as well as in the motor cortex during reaching[24], our observation in the cerebellum suggests a common principle of encoding in disparate regions of the motor system. Finally, the gain-field encoding was present if we assumed a specific anatomical organization: a cluster of Purkinje cells that projected onto a single nucleus neuron was composed of approximately equal numbers of bursting and pausing Purkinje cells, all sharing a common complex-spike property. Because the complex spikes of a Purkinje cell are due to input from the inferior olive, the gain-field encoding predicts that the oculomotor vermis is organized into clusters of Purkinje cells that share similar climbing fibre projections from the inferior olive. This, in turn, suggests that motor memories are anatomically clustered in the cerebellum by the errors that were experienced during movements[25].

1. Xu-Wilson, M., Chen-Harris, H., Zee, D. S. & Shadmehr, R. Cerebellar contributions to adaptive control of saccades in humans. *J. Neurosci.* **29,** 12930–12939 (2009).
2. Barash, S. *et al.* Saccadic dysmetria and adaptation after lesions of the cerebellar cortex. *J. Neurosci.* **19,** 10931–10939 (1999).
3. Kojima, Y., Soetedjo, R. & Fuchs, A. F. Effects of GABA agonist and antagonist injections into the oculomotor vermis on horizontal saccades. *Brain Res.* **1366,** 93–100 (2010).
4. Ohtsuka, K. & Noda, H. Discharge properties of Purkinje cells in the oculomotor vermis during visually guided saccades in the macaque monkey. *J. Neurophysiol.* **74,** 1828–1840 (1995).
5. Helmchen, C. & Büttner, U. Saccade-related Purkinje cell activity in the oculomotor vermis during spontaneous eye movements in light and darkness. *Exp. Brain Res.* **103,** 198–208 (1995).
6. Thier, P., Dicke, P. W., Haas, R. & Barash, S. Encoding of movement time by populations of cerebellar Purkinje cells. *Nature* **405,** 72–76 (2000).
7. Kase, M., Miller, D. C. & Noda, H. Discharges of Purkinje cells and mossy fibres in the cerebellar vermis of the monkey during saccadic eye movements and fixation. *J. Physiol. (Lond.)* **300,** 539–555 (1980).
8. Kojima, Y., Soetedjo, R. & Fuchs, A. F. Changes in simple spike activity of some Purkinje cells in the oculomotor vermis during saccade adaptation are appropriate to participate in motor learning. *J. Neurosci.* **30,** 3715–3727 (2010).
9. Soetedjo, R., Kojima, Y. & Fuchs, A. F. Complex spike activity in the oculomotor vermis of the cerebellum: a vectorial error signal for saccade motor learning? *J. Neurophysiol.* **100,** 1949–1966 (2008).
10. Catz, N., Dicke, P. W. & Thier, P. Cerebellar-dependent motor learning is based on pruning a Purkinje cell population response. *Proc. Natl Acad. Sci. USA* **105,** 7309–7314 (2008).
11. Catz, N., Dicke, P. W. & Thier, P. Cerebellar complex spike firing is suitable to induce as well as to stabilize motor learning. *Curr. Biol.* **15,** 2179–2189 (2005).
12. Gad, Y. P. & Anastasio, T. J. Simulating the shaping of the fastigial deep nuclear saccade command by cerebellar Purkinje cells. *Neural Netw.* **23,** 789–804 (2010).
13. Dash, S., Dicke, P. W. & Thier, P. A vermal Purkinje cell simple spike population response encodes the changes in eye movement kinematics due to smooth pursuit adaptation. *Front. Syst. Neurosci.* **7,** 3 (2013).
14. Prsa, M., Dash, S., Catz, N., Dicke, P. W. & Thier, P. Characteristics of responses of Golgi cells and mossy fibers to eye saccades and saccadic adaptation recorded from the posterior vermis of the cerebellum. *J. Neurosci.* **29,** 250–262 (2009).
15. Robinson, F. R., Straube, A. & Fuchs, A. F. Role of the caudal fastigial nucleus in saccade generation. II. Effects of muscimol inactivation. *J. Neurophysiol.* **70,** 1741–1758 (1993).
16. Fuchs, A. F., Robinson, F. R. & Straube, A. Role of the caudal fastigial nucleus in saccade generation. I. Neuronal discharge pattern. *J. Neurophysiol.* **70,** 1723–1740 (1993).
17. Person, A. L. & Raman, I. M. Purkinje neuron synchrony elicits time-locked spiking in the cerebellar nuclei. *Nature* **481,** 502–505 (2012).
18. De Zeeuw, C. I. *et al.* Spatiotemporal firing patterns in the cerebellum. *Nature Rev. Neurosci.* **12,** 327–344 (2011).
19. Telgkamp, P., Padgett, D. E., Ledoux, V. A., Woolley, C. S. & Raman, I. M. Maintenance of high-frequency transmission at Purkinje to cerebellar nuclear synapses by spillover from boutons with multiple release sites. *Neuron* **41,** 113–126 (2004).
20. Yamada, J. & Noda, H. Afferent and efferent connections of the oculomotor cerebellar vermis in the macaque monkey. *J. Comp. Neurol.* **265,** 224–241 (1987).
21. Kralj-Hans, I., Baizer, J. S., Swales, C. & Glickstein, M. Independent roles for the dorsal paraflocculus and vermal lobule VII of the cerebellum in visuomotor coordination. *Exp. Brain Res.* **177,** 209–222 (2006).
22. Krauzlis, R. J. Population coding of movement dynamics by cerebellar Purkinje cells. *Neuroreport* **11,** 1045–1050 (2000).
23. Andersen, R. A., Essick, G. K. & Siegel, R. M. Encoding of spatial location by posterior parietal neurons. *Science* **230,** 456–458 (1985).
24. Paninski, L., Shoham, S., Fellows, M. R., Hatsopoulos, N. G. & Donoghue, J. P. Superlinear population encoding of dynamic hand trajectory in primary motor cortex. *J. Neurosci.* **24,** 8551–8561 (2004).
25. Herzfeld, D. J., Vaswani, P. A., Marko, M. K. & Shadmehr, R. A memory of errors in sensorimotor learning. *Science* **345,** 1349–1353 (2014).

Author Contributions Y.K. and R.So. conceived, designed and performed all experiments. D.J.H. and R.Sh. formed the conceptual model. D.J.H. analysed the data and made all figures. R.Sh. and D.J.H. wrote the paper.

Author Information Reprints and permissions information is available at www.nature.com/reprints. The authors declare no competing financial interests. Readers are welcome to comment on the online version of the paper. Correspondence and requests for materials should be addressed to D.J.H. (dherzfe1@jhmi.edu) or R.S. (shadmehr@jhu.edu).

METHODS

No statistical methods were used to predetermine sample size.

We analysed extracellular recordings from Purkinje cells of the oculomotor vermis in five rhesus monkeys (B, F, W, K, KO) while they made saccades to visual targets[8,9] (Supplementary Information section 1). Each cell was well isolated for an average of 3,000 saccades. Briefly, a scleral search coil was surgically attached to the eye of each monkey, allowing measurement of eye position[26] while the animal's head was restrained. After surgery, the monkeys were trained to make saccades to targets of varying amplitudes and directions. We identified Purkinje cell activity in OMV by their saccade-related change in the simple-spike response, as well as the presence of complex spikes. Neurophysiological data were sampled at 50 kHz. All experiments were performed in accordance with the Guide for the Care and Use of Laboratory Animals (1997) and exceeded the minimal requirements recommended by the Institute of Laboratory Animal Resources and the Association for Assessment and Accreditation of Laboratory Animal Care International. All animal procedures were approved by the local committee at the University of Washington.

The CS-on direction for each cell was determined using the standard intra-saccadic step paradigm[27], in which the target was displaced during the initial saccade (Fig. 2). This error resulted in complex spikes during the period following the saccade, when the monkey observed the error. For every cell, we determined the CS-on direction as the error direction which elicited the largest probability of complex spikes during the 50–200 ms following the primary saccade. For $n = 39$ cells we were able to maintain excellent isolation of the Purkinje cell throughout the experiment, allowing us to perform automated identification of complex spikes on every trial. This allowed us to compute the probability of complex spikes as a function of error direction. For the remaining $n = 33$ cells, the CS-on direction was determined via analysis of the initial 50 trials for each direction of error[8]. CS-off was defined as CS-on $+180°$.

We computed firing rates by determining the inverse of the time between two consecutive simple spikes[28] and then convolved the resulting time series with a normalized Gaussian kernel with a standard deviation of 2.5 ms, which is significantly shorter than conventional kernels[6]. This guarded against overestimating the duration of a population response. We calcul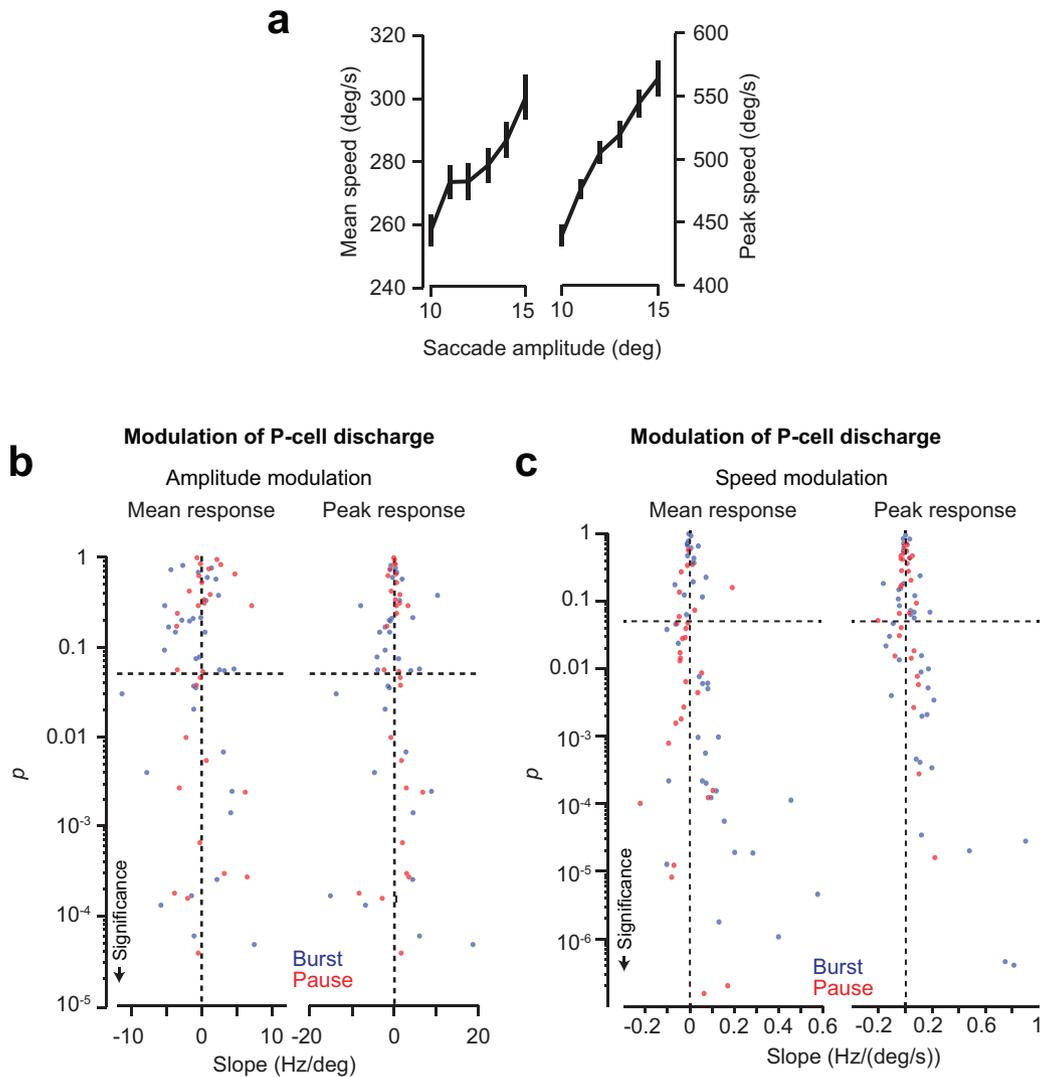ated the mean firing rate during the saccade by taking the average of the firing rate from the start to the end of the saccade. We determined the peak response of a Purkinje cell as the maximum firing during the saccade period.

The response of an individual Purkinje cell is quite variable[8], with some neurons showing a combination of bursting and pausing activity in the time period near saccade onset. Therefore, to categorize neurons exclusively as pausing or bursting, we compared the mean firing rate of each cell from the period 200–100 ms before saccade onset of all recorded trials to a 150-ms period centred on saccade peak speed. Neurons that reduced their rate during this extended period were classified as 'pausing', whereas neurons that significantly exceeded this rate were classified as 'bursting'. We tested this categorization statistically via a paired t-test with a cutoff of $P = 0.05$. Only two neurons (both bursting) did not pass this statistical test. We included these two neurons in the bursting population.

To establish confidence intervals on the population responses, we performed a bootstrap analysis in which we randomly sampled 50 neurons from the available pool of 72 (with replacement), which simulated the approximate number of Purkinje cell inputs that project onto a nucleus neuron[17]. Error bars show mean $\pm$ s.e.m. of 50 bootstrapped Purkinje cell populations. In cases where we show the responses of the bursting/pausing populations separately, we report the mean $\pm$ s.e.m. across neurons in the respective population without bootstrapping.
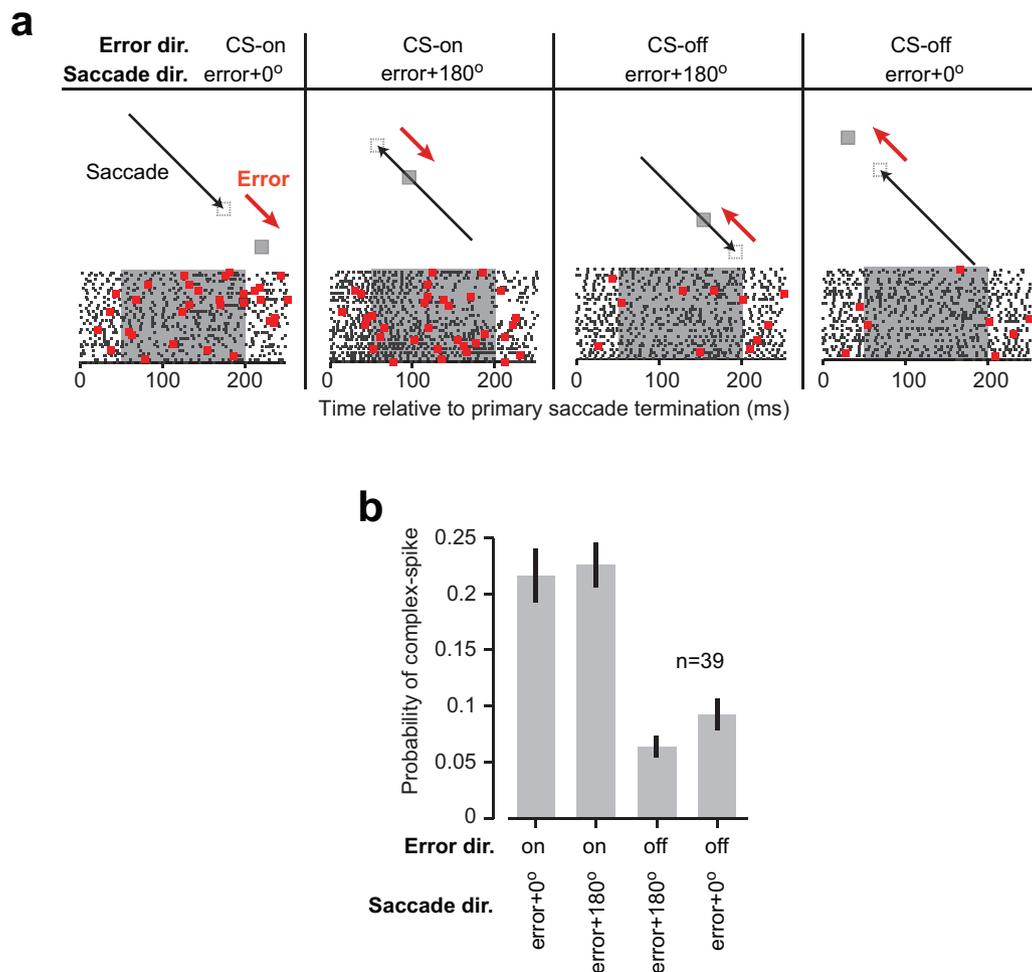
To compute the population response of a cluster of 50 Purkinje cells, we first convolved the simple spikes of each Purkinje cell with a kernel (normalized Gaussian of 2.5 ms s.d.), approximately representing the time course of post-synaptic inhibition induced by the simple-spike train[17]. We then computed the change from baseline for each cell, and finally the sum of changes across the population, resulting in a population response that had units of spikes s^{-1}, computed at each millisecond of time.

26. Fuchs, A. F. & Robinson, D. A. A method for measuring horizontal and vertical eye movement chronically in the monkey. *J. Appl. Physiol.* **21,** 1068–1070 (1966).
27. McLaughlin, S. C. Parametric adjustment in saccadic eye movements. *Percept. Psychophys.* **2,** 359–362 (1967).
28. Lisberger, S. G. & Pavelko, T. A. Vestibular signals carried by pathways subserving plasticity of the vestibulo-ocular reflex in monkeys. *J. Neurosci.* **6,** 346–354 (1986).

a

b

Modulation of P-cell discharge

Amplitude modulation

c

**Modulation of P-cell discharge**

Speed modulation

Extended Data Figure 1 | Firing rates of individual Purkinje cells as a function of saccade amplitude and peak speed. **a**, Increase in saccade amplitude produced robust increases in mean and peak saccade speed (mean: $R^2 = 0.86$, $P < 10^{-4}$; peak: $R_2 = 0.99$, $P < 10^{-9}$). Error bars indicate s.e.m. **b**, For each neuron, we correlated the average firing rate and the peak firing rate (computed over the saccade duration and averaged over all directions) with saccade amplitude. Some neurons increased their firing rates with increasing saccade amplitude (positive slope) and some neurons decreased

their responses (negative slope). However, mean and peak firing rates of a majority of neurons (47 of 72) were not significantly modulated with saccade amplitude. As a result, activity of neither the burst nor the pause cells showed a significant modulation with saccade amplitude (Fig. 1c, main manuscript). **c**, Most neurons (45 of 72) had a significant linear relationship between firing rates and peak saccade speed. In particular, mean and peak response of burst cells showed a significant increase with peak speed (Fig. 1d).

a

Error dir. Saccade dir.	CS-on error+0°	CS-on error+180°	CS-off error+180°	CS-off error+0°

Time relative to primary saccade termination (ms)

b

Extended Data Figure 2 | **Complex spikes encode direction of error, not direction of saccade that preceded that error. a**, The response of the same cell shown in Fig. 2 as a function of direction of saccade and direction of error. The probability of complex spikes is high when the direction of error is at − 45°, despite the fact that saccade direction may be at − 45° or + 135°. **b**, Population statistics from $n = 39$ Purkinje cells in which the probability of complex spikes was quantified as a function of direction of the error vector and direction of the saccade that preceded that error. Probability of complex spikes depended on direction of error, not direction of saccade.

a

All saccades (dir CS-off)

b

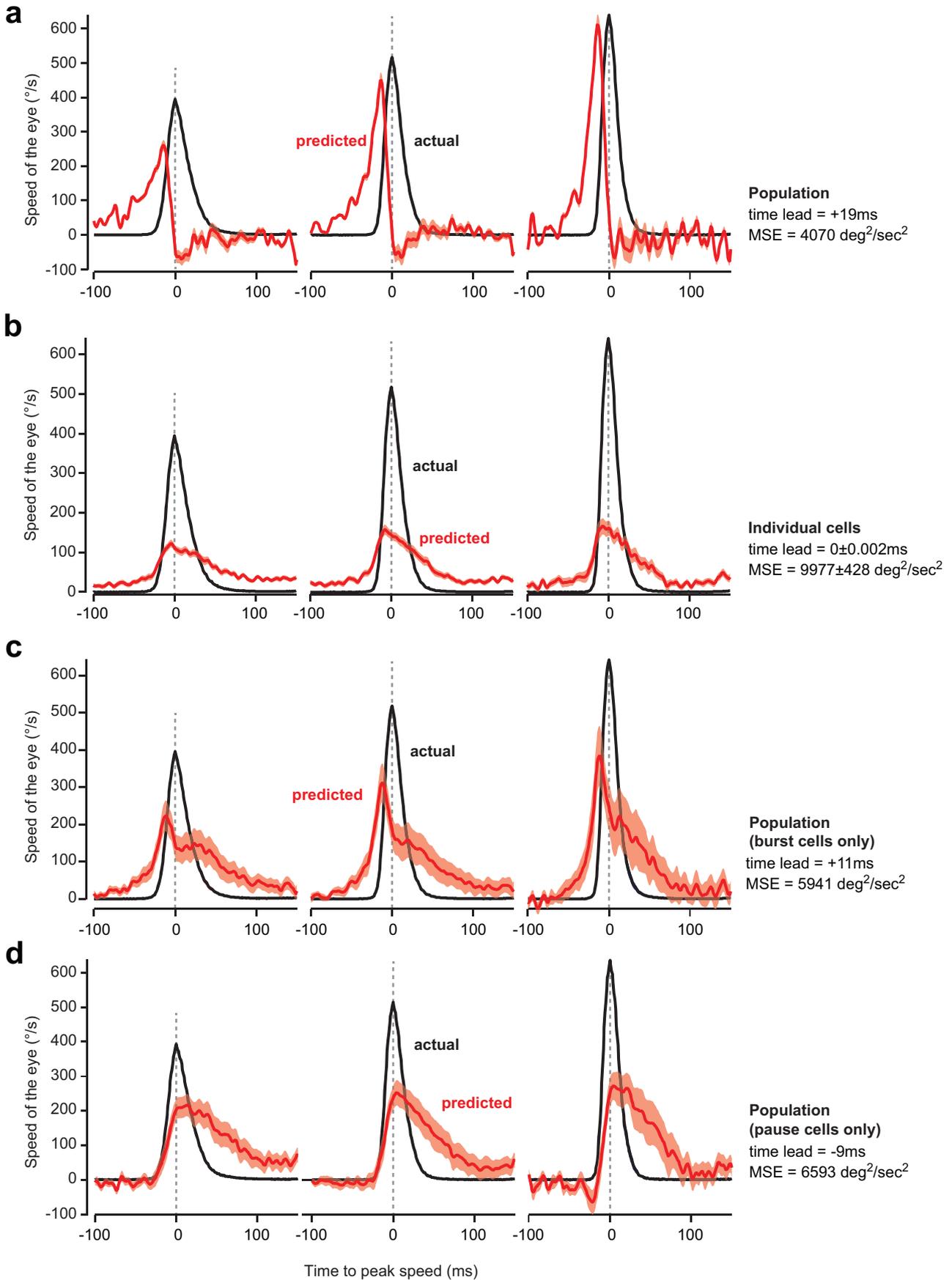All saccades (dir CS-off)

c

All saccades (dir CS-off)
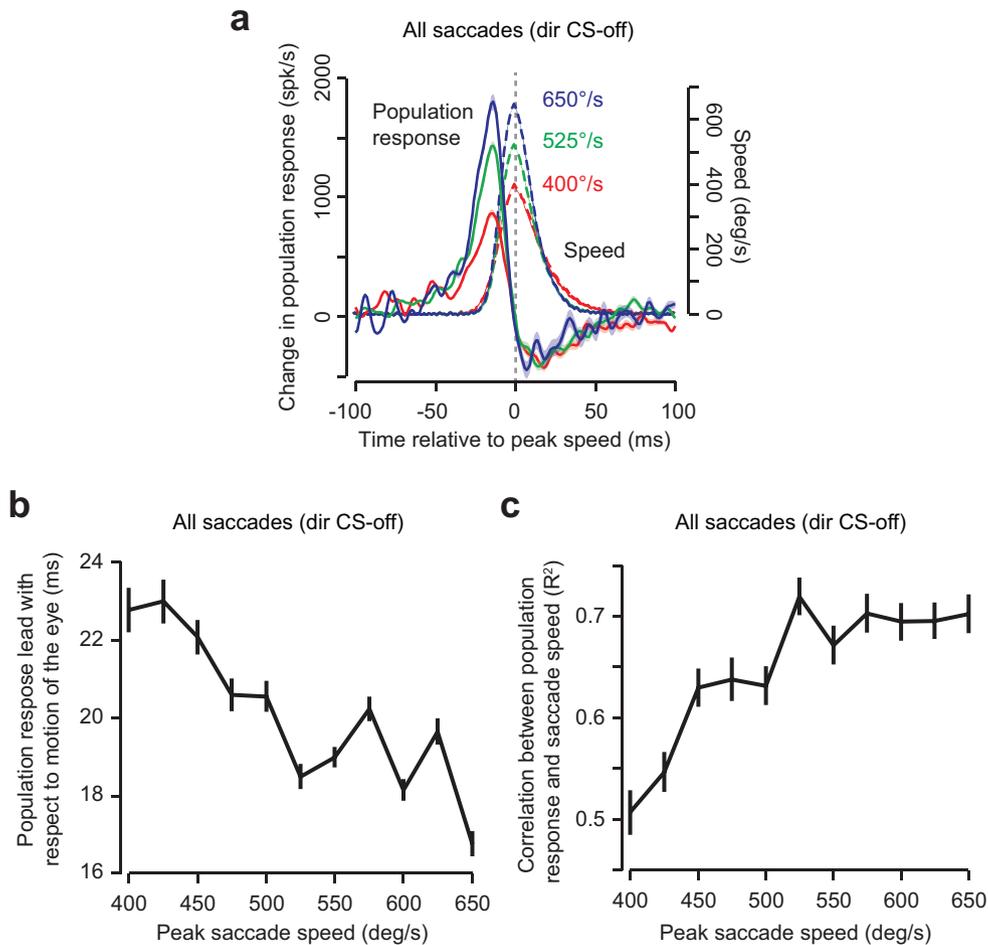
Extended Data Figure 3 | The simple-spike population response of Purkinje cells, organized by their complex-spike properties (Fig. 3a), correlated with motion of the eye in real time. a, Population response for saccades in direction CS-off for three different peak speeds. **b**, Temporal lead of the population response with respect to saccade speed as computed by finding the temporal shift that maximized the cross-correlation. **c**, Correlation between the population response and the temporally shifted eye speed trace (measured as R^2). Error bars in all panels indicate s.e.m. across bootstrapped populations.
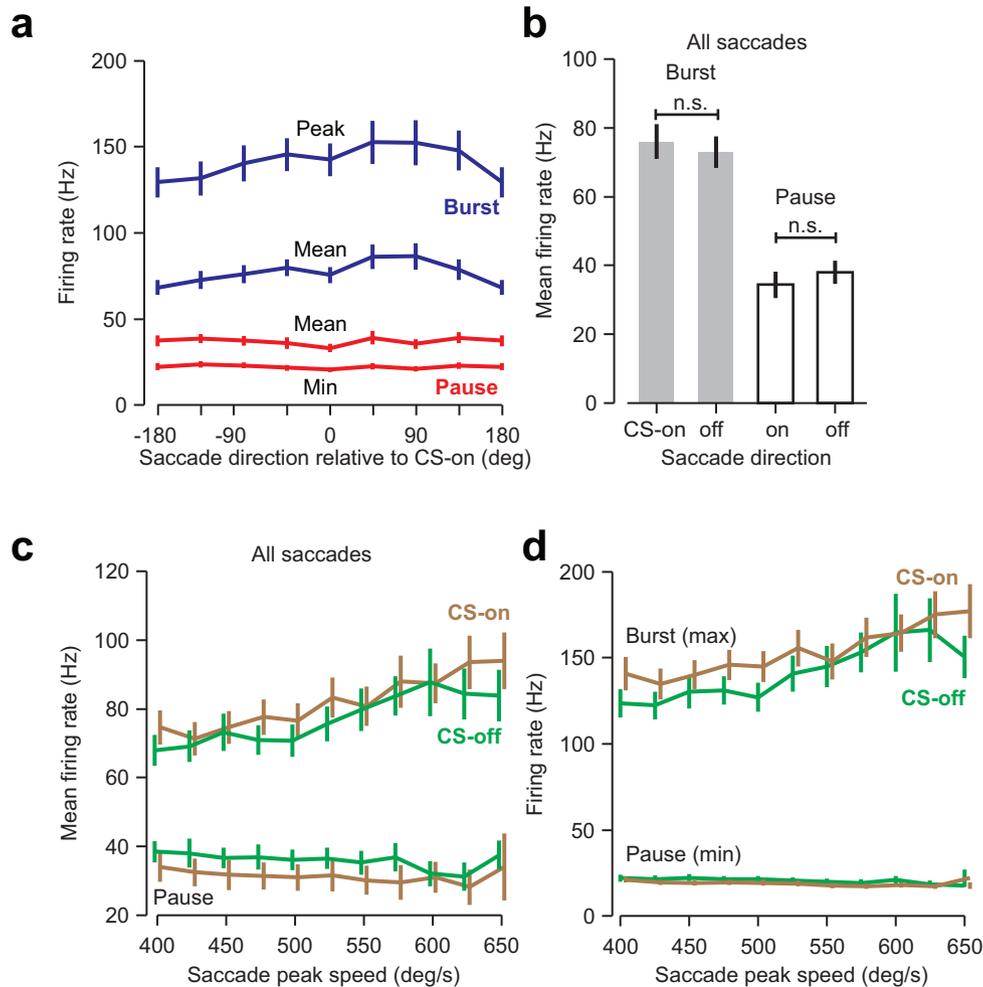
Extended Data Figure 4 | Mean and peak/trough firing rate of the burst and pause cells were poorly modulated by saccade direction. **a**, Maximum, minimum and mean firing rates averaged across burst or pause cells with respect to saccade direction, relative to CS-on direction of each cell. **b**, Mean firing rates of the burst and pause cells, as measured across all saccades, were not significantly different for saccades in the CS-on versus CS-off direction (burst $P > 0.10$, pause $P > 0.05$). **c**, Mean firing rates of the burst and pause cells as a function of saccade speed, for saccades in the CS-on versus CS-off direction. Saccade speed modulated the mean firing rates of the burst cells, but there were no significant interaction between saccade direction and speed ($P > 0.6$), nor a significant effect of saccade direction ($P > 0.7$). **d**, Peak (maximum) firing rates of the burst cells and the minimum firing rate of the pause cells as a function of saccade speed, for saccades in the CS-off and CS-on directions. We asked whether the maximum response of the burst cells or the minimum response of the pause cells was significantly modulated by direction. Separate repeated measures ANOVAs showed that for the burst cells, peak activity increased as a function of saccade peak speed ($P < 0.001$), but this relationship was unaffected by saccade direction ($P > 0.4$). For the pause cells, the response was not affected by saccade speed ($P > 0.6$), and this relationship was not modulated by saccade direction ($P > 0.4$). We found that saccade direction did not significantly alter the encoding of peak speed in either the mean or minimum/maximum activity of Purkinje cells. Error bars in all panels represent s.e.m. across neurons.

a

Speed of the eye (°/s)

predicted   actual

Population
time lead = +19ms
MSE = 4070 deg^2/sec^2

b

Speed of the eye (°/s)

actual

predicted

Individual cells
time lead = 0±0.002ms
MSE = 9977±428 deg^2/sec^2

c

Speed of the eye (°/s)

actual

predicted

**Population
(burst cells only)**
time lead = +11ms
MSE = 5941 deg^2/sec^2

d

Speed of the eye (°/s)

actual

predicted

**Population
(pause cells only)**
time lead = -9ms
MSE = 6593 deg^2/sec^2

Time to peak speed (ms)

Extended Data Figure 5 | A population of Purkinje cells, organized by their complex spike properties, predicted the real-time speed of the eye better than activity of individual cells. a, We used equation (S2) (see Supplementary Information for details) and used the measured population response $s(t)$ of Purkinje cells to predict the real-time speed of the eye $|\hat{\dot{x}}(t+\Delta)|$. The plot shows the predicted speed for saccades of 400, 525 and 650° s^{-1}. The predicted speed led the actual speed by 19 ms. MSE is the mean squared error between the predicted and actual eye trajectory at the optimal value of Δ. **b**, The result of fitting equation (S2) (see Supplementary Information) to the response of individual neurons. **c**, The result of fitting equation (S2) (Supplementary Information) to the discharge of a population composed exclusively of burst cells. **d**, The result of fitting equation (S2) (Supplementary Information) to the discharge of a population composed exclusively of pause cells.

a

b
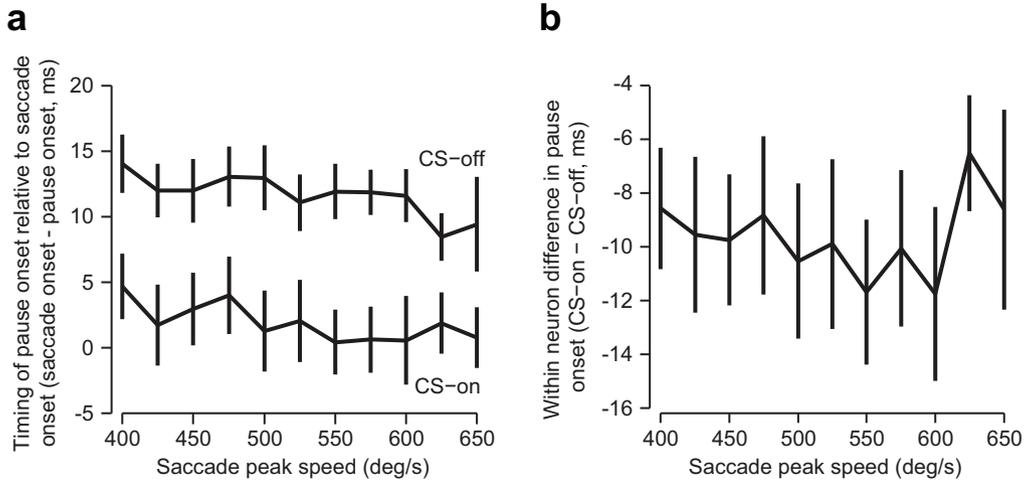
Extended Data Figure 6 | Change in saccade direction was associated with a change in the timing of the reduction of discharge in the pause cells (that is, pause onset) (see Fig. 4f). a, Timing of pause onset with respect to saccade onset for saccades of various speeds and directions. We computed the pause onset as the time when the neuron's response reached 20% of its minimum response. Positive numbers indicate that the pause onset occurred before saccade onset. **b**, Within-neuron measure of pause onset for saccade in direction CS-on, minus onset from saccades in direction CS-off. Negative numbers indicate that the pause onset occurred earlier for saccades in the CS-on direction. Error bars in all panels indicate s.e.m. across neurons.
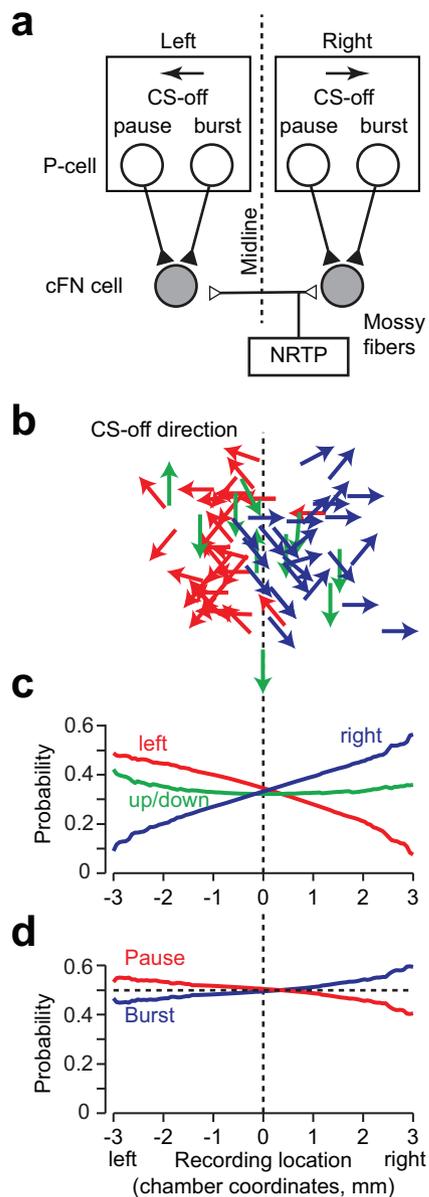
Extended Data Figure 7 | Complex-spike-dependent organization of the Purkinje cells. a, Hypothesized anatomical organization of the oculomotor vermis (OMV). Bursting and pausing Purkinje cells are organized into clusters, with the cells in each cluster sharing a common complex-spike direction. Neurons on the right side of the OMV project to right cFN neurons and have CS-off directions to the right. **b**, Distribution of the CS-off directions from recorded neurons in chamber coordinates. Vertical dotted line shows the line that best separates rightwards CS-off direction neurons (blue) from leftwards CS-off direction neurons (red). **c**, Probability of having a rightwards (blue), up/down (green), or leftwards CS-off direction as a function of chamber coordinates. Purkinje cells with CS-off to the left were more probable on the left side of the cerebellum. Purkinje cells with CS-off to the right were more probable on the right side of the cerebellum. **d**, Pause (red) and burst (blue) Purkinje cells were equally likely at all recorded locations.
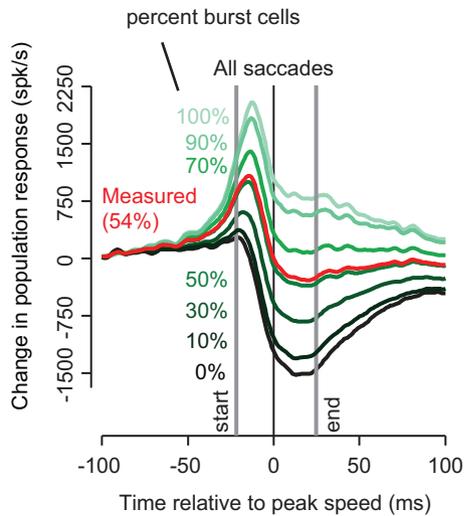
Extended Data Figure 8 | The population response was sensitive to the fraction of pause and burst cells that composed a cluster of Purkinje cells. In our data set, 54% of the population was composed of burst cells. We computed the population response under the assumption that the membership of a cluster was 54% burst cells. Here, we tested how sensitive the population response was to this membership ratio. The vertical lines indicate saccade onset and offset for all saccades pooled across direction and speed. As the percentage of burst cells in the cluster becomes larger than 70%, or smaller than 50%, the population response no longer returns to baseline at saccade offset.
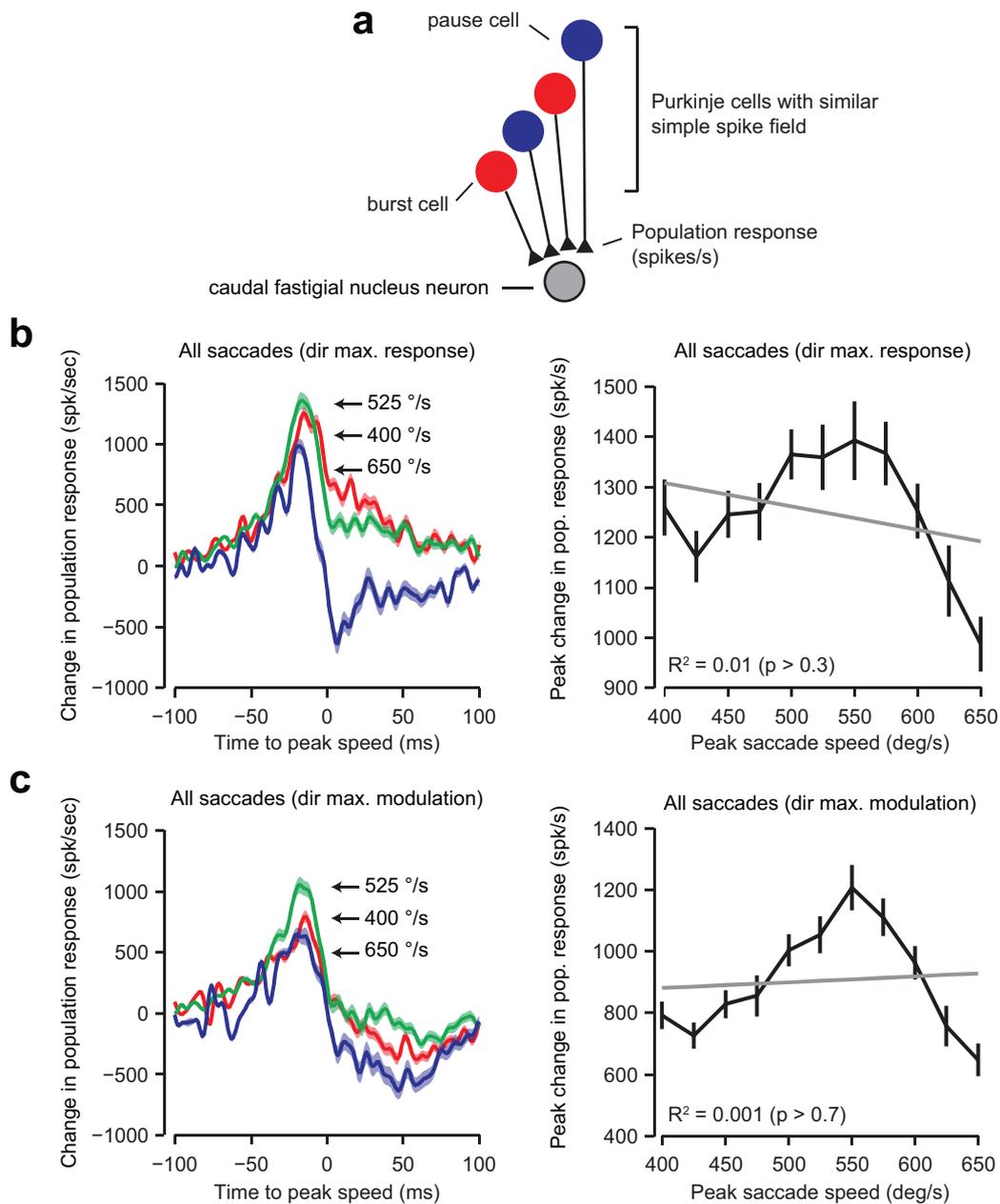
Extended Data Figure 9 | Gain-field encoding of saccade kinematics in the population response of the Purkinje cells disappeared if the Purkinje cells were organized by their simple-spike activity. a, In this analysis we assumed that a collection of 50 Purkinje cells projected onto a single cFN neuron, with the property that all the Purkinje cells shared a similar simple-spike preferred direction. Therefore, the cluster was organized based on the simple-spike properties of the Purkinje cells, not their complex-spike properties. **b**, The population response for saccades made in the direction for which each Purkinje cell showed the largest mean firing rate (simple spikes), for various saccade peak speeds. The peak population response was not modulated with saccade speed. Error bars are boot-strap-estimated s.e.m. **c**, The population response for saccades made in the direction of maximal modulation. For burst cells, this was the direction for which the Purkinje cell showed the largest mean firing rate, whereas for pause cells, this was the direction associated with the minimum activity (largest pause). The peak population response was not modulated with saccade speed when clusters were organized based on the direction of maximal simple-spike modulation.